



Molecular Mechanism of Water Evaporation

Yuki Nagata, Kota Usui, and Mischa Bonn

Max-Planck Institute for Polymer Research, Ackermannweg 10, 55128 Mainz, Germany

(Received 22 June 2015; revised manuscript received 14 October 2015; published 30 November 2015)

Evaporation is the process by which water changes from a liquid to a gas or vapor, and is a key step in Earth's water cycle. At the molecular level, evaporation requires breaking at least one very strong intermolecular bond between two water molecules at the interface. Despite the importance of this process the molecular mechanism by which an evaporating water molecule gains sufficient energy to escape from the surface has remained elusive. Here, we show, using molecular dynamics simulations at the water-air interface with polarizable classical force field models, that the high kinetic energy of the evaporated water molecule is enabled by a well-timed making and breaking of hydrogen bonds involving at least three water molecules at the interface, the recoil of which allows one of the molecules to escape. The evaporation of water is thus enabled by concerted, ultrafast hydrogen-bond dynamics of interfacial water, and follows one specific molecular pathway.

DOI: [10.1103/PhysRevLett.115.236102](https://doi.org/10.1103/PhysRevLett.115.236102)

PACS numbers: 68.03.Fg, 02.70.Ns, 64.70.F-, 82.30.Rs

Water evaporation is the phenomenon that a single water molecule and/or a cluster of water molecules completely break the hydrogen bonds (HBs) with other water molecules located in the water-air interface and move to the gas-phase region. Understanding and controlling water evaporation is essential for Earth's water cycle, saving purified drinking water and keeping the humidity constant in a closed space, as well as for chemical processes [1]. Furthermore, the rate of the evaporation has been known to affect the global climate: The evaporation of water from atmospheric aerosols controls the formation of cloud droplets, influencing the solar radiation scattering cross section of those particles [2–5]. The apparent importance of aerosols for chemical and physical atmospheric processes has stimulated much work aimed at a macroscopic understanding of droplet growth, shrinkage, and mass transport of water in and on aerosols [6–8]. These results demonstrate that molecular-level insights into the condensation and evaporation of water are critical for understanding the behavior of aqueous aerosols. The very strong intermolecular interactions that occur in water through the HBs between molecules make unusually low evaporation and high condensation coefficients compared to other, non-hydrogen bonded, liquids.

Based on these motivations, the condensation and evaporation coefficients of aqueous interfaces have been examined both experimentally [9–13] and theoretically [14–19]. Molecular dynamics (MD) studies have focused on the thermodynamics of the transition from the condensed phase to the gas phase. MD simulations combined with enhanced sampling methods have been used to show that the evaporation process can be considered as a ballistic escape from energetically stable bulk and interfacial water [16]. It has further been found that the loss of the accepted

HBs and the recognition of the first solvation shell play a critical role in the evaporation process [19]. Furthermore, Mason analyzed the MD trajectories of the water molecules evaporated from the water droplet and found that the evaporation occurs after the collision of two water molecules, in a non-HB fashion (i.e., through hydrogen-hydrogen or oxygen-oxygen interactions) [18]. Although these previous studies have addressed the detailed thermodynamics of water's evaporation, they have not provided a definitive view on how a water molecule can gain sufficient kinetic energy to move from the interface to the vacuum; the free energy of $10\text{--}12k_B T$ (25–30 kJ/mol) is required for a water molecule to move from the interface to the vacuum at room temperature [16].

In this Letter, by conducting MD simulation at the water-vapor interface, we reveal that a water molecule which will evaporate (molecule *A*) gains large momentum by colliding with another interfacial water molecule (molecule *B*) before the evaporation. Surprisingly, we found that, for evaporation of molecule *A* to occur, molecule *B* must form a HB with yet a third interfacial water molecule (molecule *C*) 44 ± 13 fs before the *A-B* collision; molecule *A* does not evaporate when this well-timed HB is not formed. It is the momentum released in the *B-C* interaction that allows *A* to escape. As such, the mechanism is reminiscent of momentum transfer in a Newton's cradle.

MD simulations were performed using an *ab initio* based polarizable and flexible POLY2VS force field water model [20]. Five-hundred water molecules were contained in a simulation cell of volume $26.6 \times 26.6 \times 160 \text{ \AA}^3$ [21]. Periodic boundary conditions were employed. We prepared 32 sets of initial coordinates and velocities. The initial velocities were adjusted to have similar total energy among these 32 systems. MD runs extending over 100 ps have

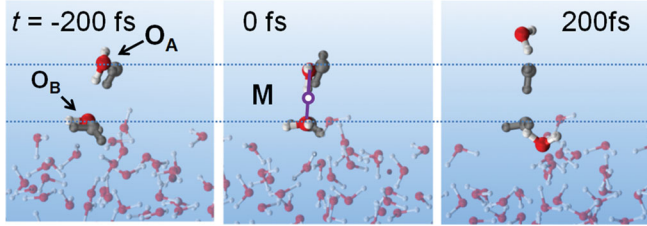


FIG. 1 (color). Snapshots of an evaporating water molecule. Molecules *A* and *B* are depicted in bold, while the other water molecules are depicted thin. The molecules with gray color indicate the water molecules 200 fs earlier. The horizontal lines are to guide the eyes.

been made in the microcanonical ensemble, allowing the systems to be equilibrated. After the equilibration, we ran 600 ps MD trajectories for these samples. The temperature averaged over the total 19.2 ns MD trajectory was 330.9 ± 1.4 K. During the MD simulations, we found 325 water molecules moving from one interface to the other interface through the vacuum region by crossing periodic boundary, which was regarded as water evaporation. We analyzed the data by investigating all 325 evaporation events. A snapshot of a typical evaporation event obtained from the MD simulation is depicted in Fig. 1. We have also performed the simulation with a nonpolarizable and rigid SPC/E model [22] to check whether our observables are universal when the different force field model is used. The details of the simulation procedure and results can be found in the Supplemental Material [23], showing that the conclusions presented here equally hold for the SPC/E model.

Before coming to the results, we briefly comment on the reliability of these models by comparing the interfacial water properties predicted from simulation with experimental observations. The SPC/E model has been frequently used as a representative model for liquid water. This water model reasonably reproduces the experimentally measured macroscopic properties of the water-vapor interface such as surface tension [31] and vapor pressure [32]. For the POLI2VS water model, its prediction of the microscopic structure of interfacial water can be tested against the surface-specific vibrational sum-frequency spectra. This model reproduces the vibrational signatures [21,33] of interfacial water molecules at the water-air interface as well as the surface tension [33]. Since the vibrational signatures are sensitive to the molecular orientation along the surface normal and HB of the interfacial water molecules, the comparison of the vibrational spectra provides a critical test for describing the microscopic structures of the interfacial water. The good agreement with experimentally measured surface tension and vibrational spectroscopic data, as well as the very similar trend of the evaporation kinetics for the SPC/E and POLI2VS water models shown below, indicate that these force field

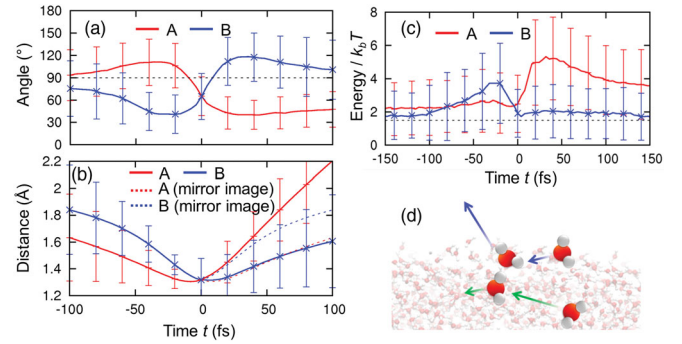


FIG. 2 (color). (a) Time evolutions of the center of mass velocity vector of molecules *A* and *B* before and after the collision. (b) Time evolutions of the r_{OA-M} and r_{OB-M} together with the time reversed (mirror) image of r_{OA-M} and r_{OB-M} for the systems. (c) Time evolutions of the kinetic energies of molecules *A* and *B*. Dotted line denotes the averaged kinetic energy. For (a), (b), and (c), the error bars represent the standard deviations of 325 events. (d) Schematic picture of the trajectories of molecules *A* (blue arrow) and *B* (green arrow).

models provide a reliable description of the interfacial water dynamics [34].

Motivated by Ref. [18], which showed that immediately prior to evaporation a final collision occurs, we analyzed the last interaction for the evaporated water molecule *A* with the surface from the MD trajectories. We define molecules *A* and *B* as follows. Molecule *A* is defined to be evaporated when it moves from one to the other interface. By tracing the MD trajectories backward in time, we can follow the molecule *A* back to the interface, to interact with interfacial water molecules. Molecule *B* is defined as the molecule that *A* last interacted with before evaporating. Details of the identification of molecule *B* can be found in the Supplemental Material [23]. For this last collisionlike *A-B* interaction, time zero was defined as the time when the distance between the oxygen atoms of molecules *A* and *B* (O_A and O_B atoms, respectively, see Fig. 1) was shortest in the MD trajectories.

To monitor the variations of the center of mass (c.m.) velocities of molecules *A* and *B*, we calculated the time evolution of the angles formed by the vector pointing from O_B to O_A atoms at $t = 0$ fs and the c.m. velocity vector of the respective water molecules. The $O_B - O_A$ vector at $t = 0$ fs is the reference axis for calculating the c.m. velocity directions. The angles averaged over the 325 evaporation events for the system are plotted in Fig. 2(a), showing that the angle of the c.m. velocity is strongly modulated between $t = -20$ to 20 fs. The instantaneous change of the angle indicates that indeed, molecules *A* and *B* collide with each other through this interaction, consistent with the previous study [18]. Before this collision the vector of the c.m. velocities of molecule *A* with respect to the $O_B - O_A$ vector was $\sim 110 \pm 30^\circ$, then molecules *A* and *B* collide and slip in a direction perpendicular to the $O_B - O_A$

vector, and the c.m. velocity of molecule *A* after the collision has similar direction of the c.m. velocity of molecule *B* before the collision. The angle changes by $\sim 75^\circ$ due to the *A-B* collision for the POLI2VS model. A very similar trend is found for the SPC/E model [Fig. S2(a) in the Supplemental Material [23]], indicating that the mechanism is independent of the water model used here.

Subsequently, we calculated the $O_A - M$ (r_{OA-M}) and $O_B - M$ (r_{OB-M}) distances as a function of time, where *M* was located at the midpoint of O_A and O_B positions at $t = 0$ fs. The time evolutions of the averaged distances are displayed in Fig. 2(b). This shows that molecule *A* moves faster after the *A-B* collision than before the collision, while the momentum of molecule *B* is dramatically reduced due to the collision. The same trend can be again seen for the SPC/E water model [Fig. S2(b) in the Supplemental Material [23]]. The observation of a time asymmetry, i.e., that $r_{OA-M}(t) \neq r_{OB-M}(-t)$ for $t > 0$, implies that this collision cannot be accounted for within the momentum conservation of only molecules *A* and *B*. Apparently, three-body effects are essential for molecule *A* to gain its unexpectedly large momentum, allowing it to move away from the interface. We also calculated the time evolution of the kinetic energy from the atom velocities, which is shown in Fig. 2(c). This indicates that the loss of the kinetic energy of molecule *B* is smaller than the gain of *A* for the collision. A schematic summary of the molecular trajectories is provided in Fig. 2(d).

To understand the mechanism by which molecule *A* gains its excess kinetic energy from other water molecules in liquid water, we explored the HB dynamics of molecules *A* and *B*. The number of HBs can be readily quantified from the simulations using the definition based on the electronic occupancies (see Ref. [36] and below). The HB number increases by 1 for each HB donated or accepted by a water molecule. Figure 3(a) shows that, for the evaporation trajectories, there is near-unity probability for a HB between *A* and *B* at $t = 0$ fs, as expected. The average HB number of

molecule *A* excluding the HB with *B*, represents a continuously decreasing function with time, from 0.5 to 0 over the 600 fs time window around the evaporation event, implying that *A* is interacting increasingly weakly with water molecules other than *B*. The smaller average HB number of molecule *A* than *B* indicates that *A* has substantially less HBs with other water molecules. Interestingly, the average HB number of molecule *B* excluding the HB with *A* peaks ~ 50 fs prior to the *A-B* collision. This shows that *B* interacts very strongly with yet a third water molecule, which we will denote as molecule *C*, at a well-determined time prior to evaporation.

While the average HB number is informative, it relies on a binary description (0 or 1). The trajectories-averaged strength of the HB is a better (because nonbinary) measure of the interactions between water molecules, and can be readily quantified by the electronic occupancy of the σ_{OH}^* antibonding orbitals between donor and acceptor [36]:

$$N(d, \psi) = \exp(-d/0.343A)(7.1 - 0.05\psi + 0.00021\psi^2). \quad (1)$$

This description relies on the HB interactions to cause electron transfer from the donor to the acceptor with electrons occupying the σ^* orbitals, resulting in the increase in *N*. As such, *N* can be considered as a suitable parameter to quantify HB interactions. *d* denotes the intermolecular $O_i \dots H_j$ distance between water molecules *i* and *j*, and ψ is the angle formed by this $O_i \dots H_j$ vector and the normal to the plane formed by water molecule *i*. The criterion whether or not a HB is formed is given, in this formalism by a HB cutoff value of 0.0085 [36], providing the data in Fig. 3(a).

The occupancy *N* of molecule *A* with all the molecules in a simulation cell except *B*, and that of molecule *B* with all the molecules except *A* are plotted in Fig. 3(b) together with the occupancy calculated from the *A-B* pair. *N* shows a similar time dependence as the average HB number, yet provides clearer peaks, as is seen from the comparison of Figs. 3(a) and 3(b). This higher time resolution, as well as the ability to quantify the HB strength, is useful to identify the dynamics of the water conformations. Therefore, hereafter, we focus on the time evolution of *N*.

First of all, it is instructive to see that the maximal electronic occupancy of the *A-B* pair achieved at $t = 0$ fs indicates that the *A-B* bond is a very strong HB. Second, the electronic occupancy of molecule *B* increases after $t = \sim -150$ fs and shows a prominent peak at $t = -44$ fs. From $t = -150$ to -44 fs, the electronic occupancy increases by $N \approx 0.0143$, i.e., much larger than the HB cutoff value of 0.0085. This means that a water molecule *C*, while not directly involved in “launching” molecule *A*, forms a HB with *B* and that the *A-B* collision is strongly correlated in time with the *B-C* HB formation. Specifically, the *B-C* electronic occupancy peaks at $t = -44$ fs. As it

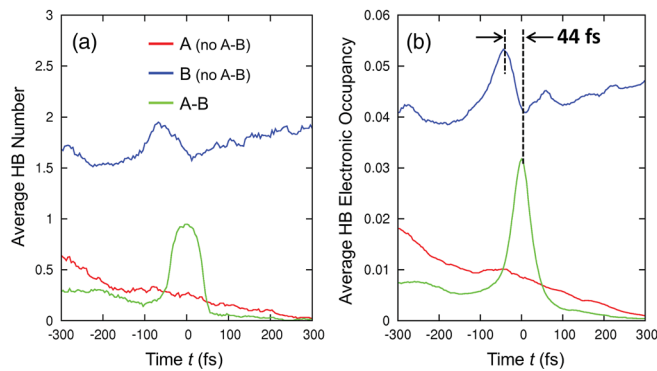


FIG. 3 (color). Time evolutions of (a) the HB number (average number of hydrogen bonds) and (b) the electronic occupancies for water molecules *A* and *B*. These are averaged over the 325 evaporation events.

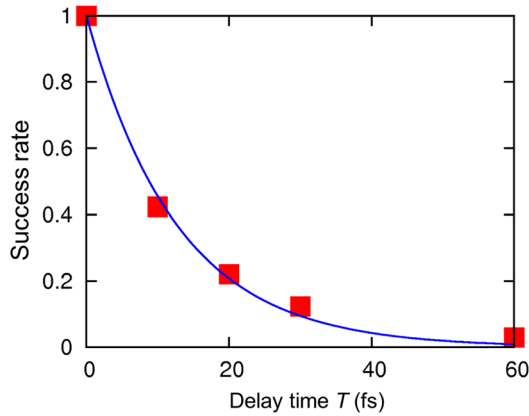


FIG. 4 (color online). Success rate for molecule A to evaporate as a function of the delay time T' , averaged over 325 evaporation events, highlighting the importance of the relative timing of A - B and B - C HB formation for the evaporation.

drops, the electronic occupancy for the A - B pair is rapidly enhanced, to peak at $t = 0$ fs. This clearly illustrates that the evaporation of A is not a simple two-body phenomenon, but is correlated with motion of molecule C , which is not hydrogen bonded to molecule A but to B , with the B - C HB strength peaking 44 fs before the A - B HB is at its strongest (at $t = 0$ fs).

To confirm the importance of the relative timing of the A - B collision and the B - C HB formation for the evaporation process, we suspended (i.e., froze) the motion of molecules A and B for a waiting time T' , from $t = -100$ to $t = -100 + T'$ fs. We chose $t = -100$ fs, because molecule B starts to gain the kinetic energy at $t = -100$ fs as shown in Fig. 2(c). Subsequently, upon “unfreezing” the water molecules at $t = -100 + T'$ fs in the MD runs, they regained their velocities at $t = -100$ fs. Simulation details can be found in the Supplemental Material [23]. The success rate for evaporation is shown as a function of waiting time T' in Fig. 4, while the variation of the electronic occupancies of molecules A and B are displayed in the Supplemental Material [23]. If the evaporation were determined only by A - B interactions, temporarily freezing molecules A and B should not greatly affect the evaporation probability. Remarkably, the evaporation success rate decays to zero with an ultrashort time constant of 13 fs. This clearly illustrates that the evaporation of molecule A is sensitive to the timing of the B - C HB formation; evaporation requires a delicately timed interplay of HB making and breaking of several molecules at the interface. Without this interplay, evaporation simply does not occur.

To elucidate why the timing of the interactions of the three water molecules governing this evaporation event is so critical, we consider a simple model with the three particles (D_1 , D_2 , D_3), each representing a water molecule, aligned along a one dimensional axis, on which the particles collide. By changing the time interval of the

$D_1 - D_2$ collision time and $D_2 - D_3$ collision time, the kinetic energy of particle D_1 before and after the collision was simulated. Note that particles D_1 , D_2 , and D_3 correspond to molecules A , B , and C , respectively. For simplicity, consider that the interaction between particles D_2 and D_3 is described by a harmonic potential, while the interaction of particles D_1 and D_2 is described by a discontinuous stepwise potential. Consider T is the oscillation period for the $D_2 - D_3$ harmonic potential. In this case, it is easy to understand that particle D_2 can transfer maximum kinetic energy to D_1 when they collide $0.25 T$ after the time when the $D_2 - D_3$ distance is minimum, since, at that moment, the momentum of D_2 is maximal. The similar results can be obtained by using anharmonic potentials (see Supplemental Material [23]). Given the known HB stretch oscillation period of $T = 180$ fs [37], our simple model predicts that molecule A can gain the maximum momentum $0.25 T \approx 45$ fs after the B - C HB formation. This is in excellent agreement with the 44 fs time delay between the A - B collision and B - C HB formation obtained from Fig. 3. This indicates that the evaporation event is dictated by the HB stretching mode and the evaporation of molecule A occurs by transferring the kinetic energy gained through the B - C HB formation to A .

Our study shows that for obtaining the additional necessary kinetic energy required for evaporation, a concerted process of the HB formation and breaking is required. Moreover, the very weak temperature dependence of the experimentally measured evaporation coefficients indicates that the entropic barrier to evaporation is possibly due to the geometric requirement of the evaporated water molecules [38]. This study accounts for this, by the concerted HB formation of the interfacial water molecules required for evaporation.

In summary, we have performed MD simulation at the water-air interface and analyzed the dynamics of the evaporated water molecules. Our simulations reveal that the large energetic barrier associated with evaporation of a water molecule from the water surface can only be overcome by a concerted, well-timed motion of several water molecules in which an instantaneous HB between two water molecules releases energy to the third, which can evaporate. Furthermore, this study indicates that by preventing the water molecules from forming HBs sequentially, the evaporation can be strongly suppressed. This points the way to the design of new surface-active molecules which suppress water evaporation.

We are grateful to Dr. Johannes Hunger, Dr. Sapun Parekh, Dr. Enrique Canovas, Mr. Seiji Yoshimune, Dr. Manabu Shiraiwa, and Dr. Toshiki Sugimoto, and Dr. Taisuke Hasegawa for fruitful discussions, and Professor Kurt Binder, Dr. John Russo, Professor Hajime Tanaka, and Professor Kurt Kremer for critical reading of the manuscript. This work was supported by the German Research Foundation (DFG) through the project of TRR146.

- [1] R. Smith, *Chemical Process: Design and Integration* (Wiley, New York, 2005).
- [2] J. F. Davies, A. E. Haddrell, R. E. H. Miles, C. R. Bull, and J. P. Reid, *J. Phys. Chem. A* **116**, 10987 (2012).
- [3] D. Rosenfeld, U. Lohmann, G. B. Raga, C. D. O. Dowd, M. Kulmala, S. Fuzzi, A. Reissell, and M. O. Andreae, *Science* **321**, 1309 (2008).
- [4] D. Rosenfeld, *Science* **287**, 1793 (2000).
- [5] C. A. Clement, R. Burgman, and J. R. Norris, *Science* **325**, 460 (2009).
- [6] J. F. Davies, R. E. H. Miles, A. E. Haddrell, and J. P. Reid, *Proc. Natl. Acad. Sci. U.S.A.* **110**, 8807 (2013).
- [7] M. Shiraiwa, M. Ammann, T. Koop, and U. Pöschl, *Proc. Natl. Acad. Sci. U.S.A.* **108**, 11003 (2011).
- [8] D. L. Bones, J. P. Reid, D. M. Lienhard, and U. K. Krieger, *Proc. Natl. Acad. Sci. U.S.A.* **109**, 11613 (2012).
- [9] E. J. Davis, *Atmos. Res.* **82**, 561 (2006).
- [10] M. Zientara, D. Jakubczyk, K. Kolwas, and M. Kolwas, *J. Phys. Chem. A* **112**, 5152 (2008).
- [11] P. M. Winkler, A. Vrtala, P. E. Wagner, M. Kulmala, K. E. J. Lehtinen, and T. Vesala, *Phys. Rev. Lett.* **93**, 075701 (2004).
- [12] P. M. Winkler, A. Vrtala, R. Rudolf, P. E. Wagner, I. Riipinen, T. Vesala, K. E. J. Lehtinen, Y. Viisanen, and M. Kulmala, *J. Geophys. Res.* **111**, D19202 (2006).
- [13] Y. Q. Li, P. Davidovits, C. E. Kolb, and D. R. Worsnop, *J. Phys. Chem. A* **105**, 10627 (2001).
- [14] J. Julin, M. Shiraiwa, R. E. H. Miles, J. P. Reid, U. Poeschl, and I. Riipinen, *J. Phys. Chem. A* **117**, 410 (2013).
- [15] R. Marek and J. Straub, *Int. J. Heat Mass Transfer* **44**, 39 (2001).
- [16] P. Varilly and D. Chandler, *J. Phys. Chem. B* **117**, 1419 (2013).
- [17] M. Schrader, P. Virnau, and K. Binder, *Phys. Rev. E* **79**, 061104 (2009).
- [18] P. E. Mason, *J. Phys. Chem. A* **115**, 6054 (2011).
- [19] N. Musolino and B. L. Trout, *J. Chem. Phys.* **138**, 134707 (2013).
- [20] T. Hasegawa and Y. Tanimura, *J. Phys. Chem. B* **115**, 5545 (2011).
- [21] Y. Nagata, C.-S. Hsieh, T. Hasegawa, J. Voll, E. H. G. Backus, and M. Bonn, *J. Phys. Chem. Lett.* **4**, 1872 (2013).
- [22] H. J. C. Berendsen, J. R. Grigera, and T. P. Straatsma, *J. Phys. Chem.* **91**, 6269 (1987).
- [23] See Supplemental Material at <http://link.aps.org/supplemental/10.1103/PhysRevLett.115.236102> for the simulation details, discussion of the evaporation rates, velocity distribution of molecule A, and a model calculation of the three-particle interaction using the Morse potential, which includes Refs. [24–30].
- [24] A. P. Willard and D. Chandler, *J. Phys. Chem. B* **114**, 1954 (2010).
- [25] H. J. C. Berendsen, J. R. Grigera, and T. P. Straatsma, *J. Phys. Chem.* **91**, 6269 (1987).
- [26] The CP2K developers group, <http://www.cp2k.org/>.
- [27] W. L. Jorgensen, J. Chandrasekhar, J. D. Madura, R. W. Impey, and M. L. Klein, *J. Chem. Phys.* **79**, 926 (1983).
- [28] Y. Wu, H. L. Tepper, and G. A. Voth, *J. Chem. Phys.* **124**, 024503 (2006).
- [29] R. D. Present, *Kinetic Theory of Gases* (McGraw-Hill, New York, 1958).
- [30] W. Wagner and A. Pruss, *J. Phys. Chem. Ref. Data* **22**, 783 (1993).
- [31] C. Vega and E. De Miguel, *J. Chem. Phys.* **126**, 154707 (2007).
- [32] J. R. Errington and A. Z. Panagiotopoulos, *J. Phys. Chem. B* **102**, 7470 (1998).
- [33] Y. Nagata, T. Hasegawa, E. H. G. Backus, K. Usui, S. Yoshimune, T. Ohto, and M. Bonn, *Phys. Chem. Chem. Phys.* **17**, 23559 (2015); T. Ohto, K. Usui, T. Hasegawa, M. Bonn, and Y. Nagata, *J. Chem. Phys.* **143**, 124702 (2015).
- [34] In our current, fully classical simulation, possible effects of nuclear quantum effects are missing. However, the evaporation coefficients of H₂O and D₂O are identical within the error bar [35], implying that the nuclear quantum effects are not dominant for evaporation process. Thus, it can be reasonably assumed that the nuclear quantum effects do not modify the kinetics of water evaporation described here.
- [35] W. S. Drisdell, C. D. Cappa, J. D. Smith, R. J. Saykally, and R. C. Cohen, *Atoms. Chem. Phys.* **8**, 6699 (2008).
- [36] R. Kumar, J. R. Schmidt, and J. L. Skinner, *J. Chem. Phys.* **126**, 204107 (2007).
- [37] C. Fecko, J. Eaves, J. Loparo, A. Tokmakoff, and P. Geissler, *Science* **301**, 1698 (2003).
- [38] J. D. Smith, C. D. Cappa, W. S. Drisdell, R. C. Cohen, and R. J. Saykally, *J. Am. Chem. Soc.* **128**, 12892 (2006).